World Journal of Radiology

Online Submissions: http://www.wjgnet.com/1949-8470office
wjr@wjgnet.com
doi:10.4329/wjr.v2.i4.135

World J Radiol 2010 April 28; 2(4): 135-142
ISSN 1949-8470 (online)

REVIEW

Proton therapy dosimetry using positron emission tomography

Matthew T Studenski, Ying Xiao

Matthew T Studenski, Ying Xiao, Bodine Cancer Center, Department of Radiation Oncology, Thomas Jefferson University Hospital, 111 S. 11th St., Room G-321 Gibbon Building, Philadelphia, PA 19107, United States
Author contributions: Studenski MT wrote the paper; Xiao Y reviewed and edited the paper.
Correspondence to: Matthew T Studenski, PhD, Bodine Cancer Center, Department of Radiation Oncology, Thomas Jefferson University Hospital, 111 S. 11th St., Room G-321 Gibbon Building, Philadelphia, PA 19107,
United States. matthew.studenski@Jeffersonhospital.org
Telephone: +1-215-9550300 Fax: +1-215-9550412
Received: March 11, 2010 Revised: April 1, 2010
Accepted: April 12, 2010
Published online: April 28, 2010

Abstract

Protons deposit most of their kinetic energy at the end of their path with no energy deposition beyond the range, making proton therapy a valuable option for treating tumors while sparing surrounding tissues. It is imperative to know the location of the dose deposition to ensure the tumor, and not healthy tissue, is being irradiated. To be able to extract this information in a clinical situation, an accurate dosimetry measurement system is required. There are currently two *in vivo* methods that are being used for proton therapy dosimetry: (1) online or in-beam monitoring and (2) offline monitoring, both using positron emission tomography (PET) systems. The theory behind using PET is that protons experience inelastic collisions with atoms in tissues resulting in nuclear reactions creating positron emitters. By acquiring a PET image following treatment, the location of the positron emitters in the patient, and therefore the path of the proton beam, can be determined. Coupling the information from the PET image with the patient's anatomy, it is possible to monitor the location of the tumor and the location of the dose deposition. This review summarizes current research investigating both of these methods with promising results and reviews the limitations along with the advantages of each method.

Key words: Positron emission tomography; Proton therapy; Dosimetry

Peer reviewers: Tove J Grönroos, PhD, Adjunct Professor, Turku PET Centre, Preclinical Imaging/Medicity Research Laboratory, Tykistokatu 6A, FI-20520 Turku, Finland; Sandip Basu, MBBS (Hons), DRM, DNB, MNAMS, Head, Nuclear Medicine Academic Programme, Radiation Medicine Centre, Bhabha Atomic Research Centre, Tata Memorial Hospital Annexe, Parel, Bombay 400012, India; Filippo Cademartiri, MD, PhD, Departmento of Radiology - c/o Piastra Tecnica - Piano 0, Azienda Ospedaliero-Universitaria di Parma, Via Gramsci, 14 - 43100 Parma, Italy

Studenski MT, Xiao Y. Proton therapy dosimetry using positron emission tomography. *World J Radiol* 2010; 2(4): 135-142 Available from: URL: http://www.wjgnet.com/1949-8470/full/v2/i4/135.htm DOI: http://dx.doi.org/10.4329/wjr.v2.i4.135

INTRODUCTION

Radiation can be delivered to kill tumors in a variety of ways. Treatments range from brachytherapy (implanting a radioactive seed in the tumor), to radioactively tagged molecules that are injected into the patient and are uptaken into the tumor, to external X-ray and electron beam treatments using linear accelerators or radioactive isotopes, to heavy ions produced in cyclotrons or synchrotrons. All of these therapies are used clinically but proton therapy is becoming more and more popular due to the unique dose deposition of heavy charged particles. Protons deposit almost all of their energy at the end of their path, called the Bragg peak, and therefore it is imperative that this Bragg peak is located in the tumor and not in healthy tissue.

As the power of proton therapy to treat cancer is recognized, new facilities are being constructed and commissioned worldwide. However, there are currently many unanswered questions regarding proton therapy. One of

the most important unknowns is the uncertainty in the location of the dose deposition. Knowing this location exactly is difficult due to internal motion of the patient's organs and the changing anatomy of the tumor over a course of radiation therapy. Furthermore, the range of the proton is uncertain due to tissue inhomogeneities and complications in modeling proton transport. It is essential to have a dosimetry system that can relate the location of the proton dose deposition to the patient's anatomy at the time of treatment for verification as well as for adaptation of the treatment plan as needed.

Investigation into devices like thermoluminescent dosimeters[1-4] to measure the dose from proton therapy shows potential but the emerging trend for *in vivo* proton therapy dosimetry is positron emission tomography (PET)[5-11]. The theory is that, as the protons enter the patient, they undergo inelastic collisions with atoms in tissues, which result in nuclear reactions producing positron emitters[12]. The PET system can detect the annihilation photons produced in the patient and therefore the location of the proton beam can be established and then related to the patient's anatomy.

PROTON THERAPY

History

Proton therapy was first suggested by Harvard physicist Robert Wilson in 1946[13]. Wilson went on to support his idea by showing that proton therapy can place the maximum radiation dose in the tumor without harming surrounding tissues. He also showed that for larger tumors, the normally narrow Bragg peak can be spread out using a modulator wheel. Following this publication, research on proton therapy began. In 1954, the first proton therapy treatment was performed on a pituitary tumor and, by 1958, proton therapy was widely accepted as a neurosurgery tool[14].

Theory

The physics of proton energy deposition is the driving factor for their use in radiation therapy as opposed to photons. The depth dose curve for photons follows a buildup region, a peak at a depth where the dose is at a maximum, and a long tail as the depth increases as seen in Figure 1. The shape of this curve is result of the exponential attenuation of photons in a medium[15]. Photons are indirectly ionizing radiation, that is, they must transfer energy to other charged particles, like electrons, which then deposit dose. Since one goal of radiation therapy is to spare healthy tissue, the exponential tail is undesirable because it will deposit dose in healthy tissues after passing through the tumor. Furthermore, the depth of the maximum dose is relatively fixed near the surface of the patient so treating deep tumors is inefficient since the maximum dose cannot be located on the tumor.

Protons are directly ionizing charged particles. Charged particles deposit energy through four interactions; (1) inelastic collisions with atomic electrons; (2) inelastic collisions with the nucleus; (3) elastic collisions with atomic electrons; and (4) elastic collisions with the nucleus[15]. Protons are considered heavy charged particles (opposed to electrons or positrons, which are light). The path of protons tends to be straight and the energy deposited (E) along the path ds can be calculated using Eq. 1[15].

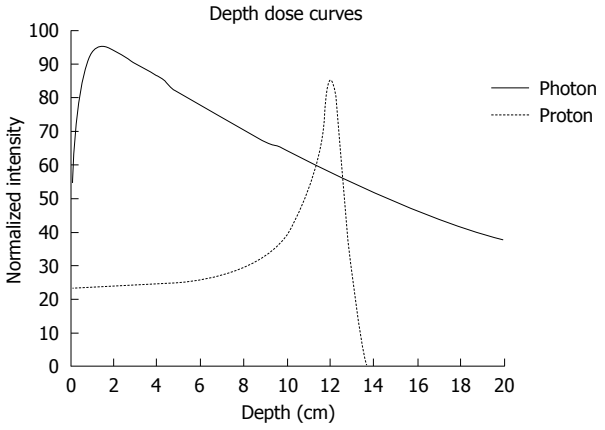

Figure 1 Depth dose curves for photons and protons. Notice the exponential tail seen in the photon curve that results in dose deposition through the entire patient. The proton curve shows that there is no dose deposition after the Bragg peak.

Eq. 1:

$$\frac{dE}{ds} = \frac{4\pi e^4 z^2}{m_0 V^2} NZ\left[\ln\frac{2m_0V^2}{I} - \ln\left(1-\beta^2\right) - \beta^2\right]$$

In this equation, the proton has charge ze, velocity $V = \beta c$, in a medium of N atoms/cm^3 and atomic number Z, and ionizing potential I.

Eq. 1 shows that the energy of the proton is constantly decreasing as it traverses through a medium. As the energy decreases, the amount of ionization per unit length increases[16]. The result of this is that most of the proton's energy is deposited at the end of the path in a region called the Bragg peak. The difference between proton dose deposition and that of photons can been seen in the depth dose profiles in Figure 1. The shape of the Bragg peak is determined by the average ionization per unit length $I(r)$ as defined in Eq. 2[15].

Eq. 2:

$$I(r) = \int_r^\infty \frac{i(x-r)}{\alpha\sqrt{\pi}} e^{-[(x-R)/\alpha]^2} dx$$

In Eq. 2, r is the distance from the source, x is the range of an individual particle, $i(x-r)$ is the specific ionization along the path of an individual particle at a distance $(x-r)$ from the end of its path, and a is the range straggling parameter.

As seen in Figure 1, the Bragg peak is the driving force behind using protons for radiation therapy because beyond the range of the proton, there is no more ionization and therefore no more dose deposition. In addition, the depth of the Bragg peak is energy dependent and therefore the location of the dose deposition can be controlled to be directly on the tumor. The Bragg peak can be spread out through modulation to treat larger

tumors. The overall result of this is a higher dose to the tumor with a reduced dose to the surrounding healthy tissue.

Problems

There are several issues with proton therapy that are currently under investigation. One of these is the lateral penumbra that results from the spread of the beam from proton scatterings in the modulator wheel, the aperture, the bolus, and in the patient. This causes protons to lose energy and have trajectories that are different than expected, widening the beam by as much as a few millimeters[17,18].

A second issue is that the treatment planning is done using a computed tomography (CT) scan to determine stopping powers in the different tissues for the protons. The CT images have pixels that are in Hounsfield units, which can then be related to electron density in tissue. Because of the errors in converting between Hounsfield units and proton stopping power, the expected range of the protons for treatment plans based on Hounsfield units can have errors up to several mm in bone and soft tissue[19-21].

Other uncertainties in proton therapy result from the treatment planning. There are three methods of treatment planning: ray-tracing, pencil beam approximation[22], and Monte Carlo simulations. The fastest is simple ray-tracing but this is very susceptible to errors from tissue inhomogeneities and at tissue interfaces. The pencil beam approximation is more accurate but this method only convolves functions that represent the incident beam and the scattering conditions so there is still uncertainty in the result. The most accurate is a Monte Carlo simulation, but this is extremely time consuming. However, physical processes like nuclear fragmentation and energy loss straggling can be ignored to reduce computation time. With the rapid advancement of computing technology, the speed may become less of an issue.

One of the most important issues is that of accurate delivery of dose to the patient[23]. This depends both on the delivery of the beam and monitoring the changes in patient anatomy from motion or deformations of targets and structures between treatments. If one can accurately monitor the dose delivered to the patient, the dose to the tumor and surrounding tissues can be measured and modified, if necessary. One of the most promising methods of dosimetry for proton therapy is to use PET imaging to track the positron emitters created from inelastic nuclear collisions of protons with the elements in tissues.

PET FOR PROTON THERAPY DOSIMETRY

As stated above, the rational behind using PET for dosimetry is that as the protons enter the patient and interact with the elements in tissue, there are inelastic collisions that produce positron emitters. The positron emitters are only produced in very small quantities and are short lived, but the detected signal is strong enough to be used as a method for dosimetry. Table 1 shows the main isotopes produced by inelastic collisions of protons in tissue.

Table 1 Relevant positron emitter reactions in tissue from proton therapy

Reaction	Threshold energy (MeV)	Half life (min)	Positron energy (MeV)
$^{16}O(p, pn)^{15}O$	16.79	2.037	1.72
$^{16}O(p, \alpha)^{13}N$	5.66	9.965	1.19
$^{14}N(p, pn)^{13}N$	11.44	9.965	1.19
$^{12}C(p, pn)^{11}C$	20.61	20.390	0.96
$^{14}N(p, \alpha)^{11}C$	3.22	20.390	0.96
$^{16}O(p, \alpha pn)^{11}C$	59.64	20.390	0.96

The image obtained from a PET scan after proton therapy is essentially the negative of the dose deposited[8,10]. Because of the energy dependence of the reaction cross sections, the inelastic scattering nuclear reactions tend to occur at higher proton energies than at the proton energies associated with the Bragg peak. Because of this, at the Bragg peak, the concentration of the positron emitters rapidly decreases because energy deposition happens through other interactions, not inelastic collisions. Therefore, the PET image shows activity up to the Bragg peak and then falls off, which is extremely important because the location of the Bragg peak can then be determined.

Due to scatterings in the beam delivery system, patient motion, and changes in the anatomy of the patient throughout treatment, an ideal treatment delivery can be difficult to achieve. The activity distribution of the positron emitters seen in the PET images provides information on where the dose was actually delivered for that particular treatment. By tracking the delivered dose from fraction to fraction, the treatment plan can be modified as needed to ensure the dose is delivered to the tumor.

There are two ways to acquire a PET image from proton therapy for dosimetry. The first of these is what is called in-beam or online PET monitoring. This method consists of a small field-of-view dual head PET system that is physically attached to the proton gantry as seen in Figure 2[24]. The advantage of this approach is that the acquisitions are performed during or very soon after the treatment so there is minimal decay from the short lived positron emitters. Also, the patient remains in the treatment position so there is no anatomical shifting.

The second approach is called offline monitoring and the patient is moved following treatment to a dedicated PET/CT scanner. This transfer can take up to 30 min during which many of the positron emitters have decayed or been transported away from their original location by the circulatory or lymphatic system in a process called biological washout. On the other hand, the image acquired on the dedicated PET/CT scanner is easily fused to obtain anatomical information and the sensitivity and spatial resolution is improved. Both approaches are cur-

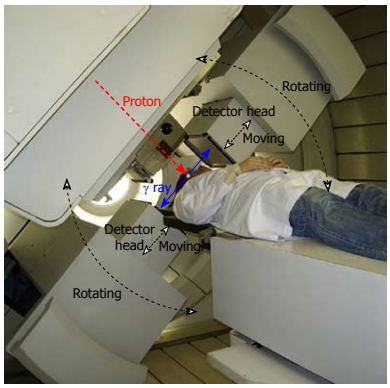

Figure 2 Setup of the on-line positron emission tomography (PET) system mounted on the rotating proton gantry. The proton beam direction is shown by the red line and the direction of the detected annihilation photons is shown in blue. (Reprinted from[24] with permission from Elsevier Limited).

rently under investigation and show promising results in proton therapy dosimetry.

Online monitoring

Online monitoring of positron emitters for radiation therapy was introduced in the late 1990s for carbon ion therapy[25,26]. More recently, two groups have applied this method to proton therapy. The first group, led by Parodi K, focused mainly on the feasibility of this approach for proton therapy. The investigators compared the activity distributions of positron emitters from carbon therapy and proton therapy[27,28]. In carbon therapy, because of the interaction of the heavier carbon ions, spallation products form a peak of activity very close to the actual Bragg peak. With protons, the activity distribution is constant as the beam enters the patient and falls off at the Bragg peak (due to the dependence of the reaction cross section on energy). Although it was not as easy as using the activity peak as with carbon therapy, it was found that there was a correlation between the 50% level of the fall-off region and the location of the Bragg peak. There was also good agreement with the lateral spread of the beam. The greatest advantage of the on-line system was that the acquisition was performed immediately following treatment reducing both the decay of the short lived isotopes and also the effect of biological washout.

The second group, led by Nishio T, also performed preliminary studies with their system and found the results to be satisfactory[29]. Along with the reduced decay and biological washout, it was found to be much easier to perform daily PET imaging with the online system. With this in mind, a workflow for quality assurance was developed where a daily PET image was acquired and compared to the initial PET image (Figure 3[24]). It was found that as treatment progressed, the tumor would shrink and the patient's anatomy would change. This change resulted in a deformation of the activity distribution from the initial plan. When this deviation in the daily PET image was found, the patient would be replanned to account for the change in the anatomy. This workflow was put into clinical practice and the results were analyzed for 48 patients with tumors in the head and neck, liver, lungs, prostate, and brain[24]. The daily monitoring showed that reduction in the head and neck tumors changed the dose distribution and the plans were adjusted accordingly. It was also found that biological washout of the positron emitters in liver cells was slower in necrotic cells than in non-necrotic cells. Overall, this method of daily, online monitoring of the dose distribution from proton therapy was confirmed as feasible in a clinical environment.

Although this method shows promise for proton therapy dosimetry, disadvantages of using the on-line system include reduced sensitivity of the detectors, a small field of view, and geometrical problems from the orientation of the beam and the detectors interferes with 3D image acquisition[26,30,31]. The reduced sensitivity and small field of view are in relationship to a dedicated PET system since in a dedicated system, there are essentially multiple opposed detector heads forming a ring around the patient, increasing both sensitivity and field of view size. Furthermore, anatomical images are not obtained daily with the online system. Nishio mentions that the addition of daily cone-beam CT would alleviate this problem.

Offline monitoring

As with the on-line systems, initial research using an offline PET/CT scanner following proton therapy showed promise for clinical investigation[17,18,32,33]. The problem faced with this method is the time required to move the patient from the treatment room to the PET/CT scanner resulting in time for decay causing loss of signal, biological washout, and anatomical motion, depending on the treatment site. The loss in signal from decay is partially offset by the high sensitivity and spatial resolution of new PET/CT systems and that the field-of-view is much larger. Another advantage of the PET/CT scanner is the ease of fusing anatomical information to the activity image. Performing a full CT scan before the PET scan allows for accurate attenuation corrections and a co-registered image to be used with the PET scan.

Three clinical studies have recently been completed using the offline approach for dosimetry[34-36]. The group led by Nishio T studied about 20 patients undergoing proton therapy to the brain, head and neck, liver, lungs, and sacrum. One focus of this study was the effect of the biological washout of the positron emitters during the time it took to transport the patient to the PET/CT scanner. This motivation was spurred by the group's research into the on-line PET method. Upon visual inspection of the activity images following treatment of the different sites, it was found that activity conformed well to the planned treatment area (treatment depth and lateral spread). The highest activity was found in adipose tissue and in bone. To quantify this observation, three points were taken for each site of interest, one in the

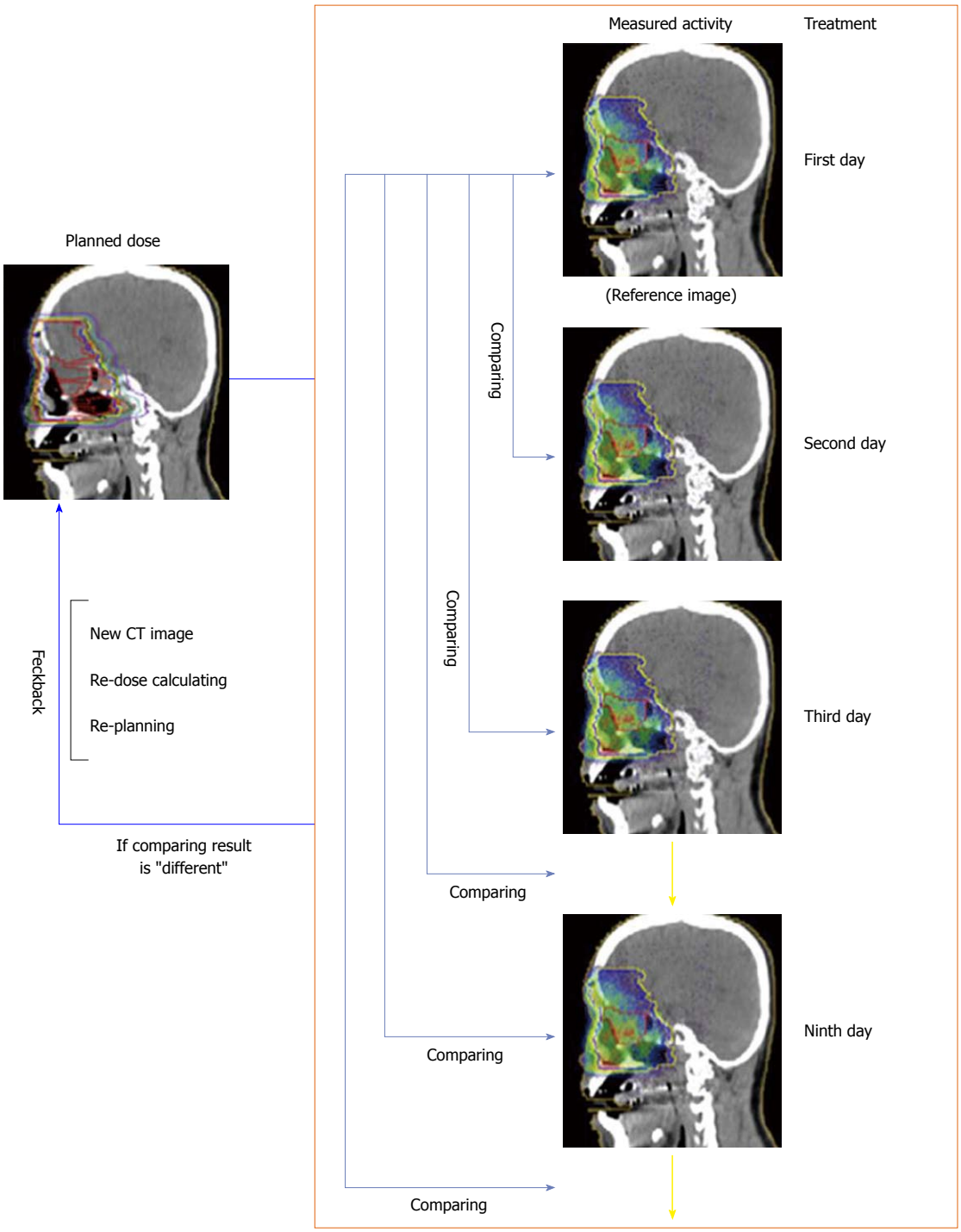

Figure 3 Flow diagram of the procedure for the clinical use of an on-line PET system (Reprinted from[24] with permission from Elsevier Limited).

soft tissue (or tumor), one in the adipose tissue, and one in the bone tissue. The measured activity was compared to both a calculated activity based on tissue composition, decay, and biological washout effects, and to a simulation of the activity that would be obtained with an on-line system immediately following treatment. Results showed good agreement between the measured and calculated activity in soft tissue, an increase of two to four in the calculated adipose tissue activity, and an increase of two times the activity in bone. The increase in activity was believed to be a result of inaccurate attenuation corrections for the adipose tissue near the surface and the increase in bone tissue was believed to be from inaccuracies in the Ca-40 fragmentation cross section. The simulation of using an on-line system showed losses in activity intensity from transportation to the offline system of up to 75%, depending on the type of tissue. Also, it was found that the effect of biological washout was lower than the previously estimated 50%-65%, although the overall effect was not quantified[37,38].

The study led by Parodi K took nine patients with different types of head and neck cancers and used a PET/

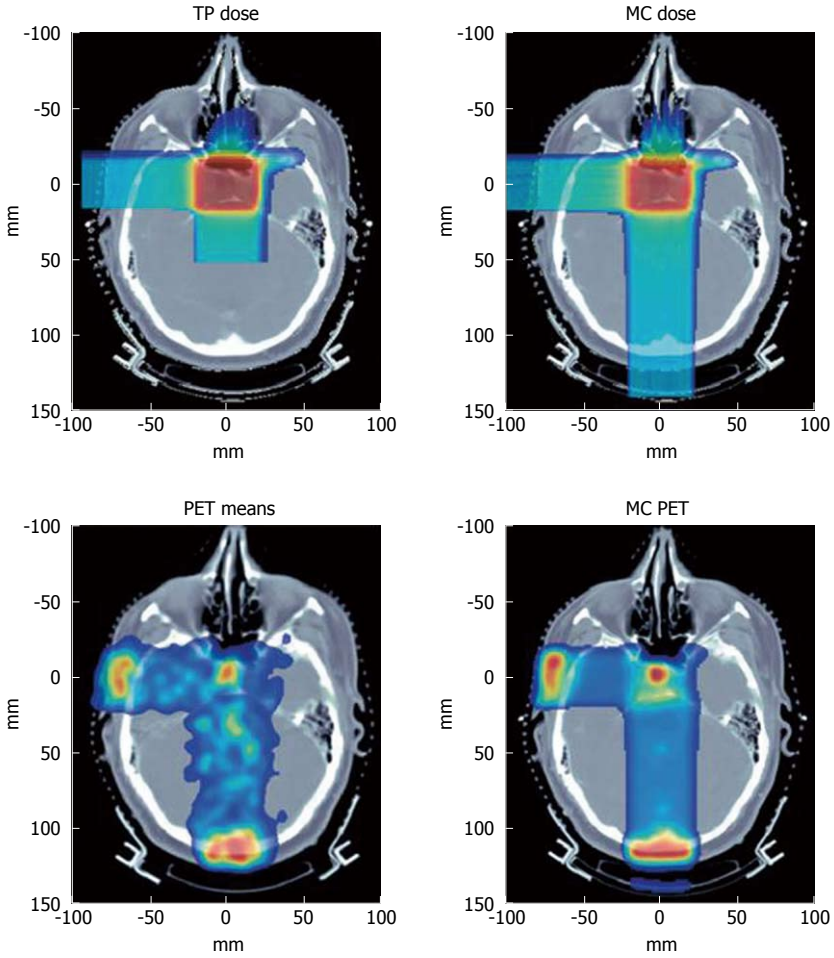

Figure 4 Top: Treatment plan (TP) and Monte Carlo (MC) dose for a patient with pituitary adenoma receiving two orthogonal fields. Bottom: Measured and Monte Carlo PET images. Delay times from the beginning of imaging were about 26 and 18 min from the end of the first and second field applications, respectively. Range of color wash is from blue (minimum) to red (maximum) (Reprinted from[34] with permission from Elsevier Limited).

CT system to verify the dose to the patient with the motivation that an on-line system can only be used for a visual inspection of dose deposition since the activity is not directly proportional to the dose. In this study, the measured activity from the offline PET scan was compared to the expected activity distribution calculated using the FLUKA Monte Carlo code accounting for biological decay and image formation[39]. The results from a patient with a pituitary adenoma can be seen in Figure 4[34]. With this method, range monitoring of proton depth was accurate to within 2 mm. As with the study by T. Nishio, the biological washout in different tissues was also examined. It was found that there was reduced biological decay in adipose tissue and bone and increased perfusion throughout the muscle and brain. Overall, this method was shown to be feasible for clinical *in vivo* dosimetry following proton therapy and it was suggested that new technology such as time-of-flight PET and new filtering methods to account for activity distributions over time could further improve this technique[40,41].

The final study led by Hsi W and Indelicato D acquired 50 PET/CT imaging studies on 10 different prostate cancer patients[36]. Instead of trying to quantify the dose delivered, this study defined the activity seen in the pelvic bone as the PET-defined beam path and compared this to the marker-defined beam path, which was calculated from seeds implanted in the prostate. The pelvic bone was chosen as the anatomical landmark to reduce the activity inhomogeneities seen in other tissues. The goal was to determine if the margins (4 mm axial, 6 mm superior and inferior perpendicular to the beam path, 7 mm proximal to the beam path, and 5 mm distal to the beam path) used for treatment were sufficient to account for prostate motion throughout treatment. The deviations between the PET-defined path and the marker-defined path were analyzed for these 10 patients. The images from one patient are seen in Figure 5[36]. Results of this study showed that with the proper immobilization device, less than 2° of angular rotation was seen for all patients. The motion of the prostate was also traced in the superior-inferior direction and in the anterior-posterior direction. It was found that for 30 of the 50 cases, motion in both of those directions was less than 6 mm, meaning that the planning margins were sufficient. For the other 20 cases, 13 of these were considered motion-after-treatment cases where large volumes of rectal gas caused prostate motion of more than 6 mm in any direction. The final seven cases were deemed position-error cases which showed no misalignment but the prostate moved more than 6 mm. These cases showed that there was either an error in positioning the patient or the prostate moved after positioning but before the proton beam was turned on.

This study demonstrated that the accepted clinical

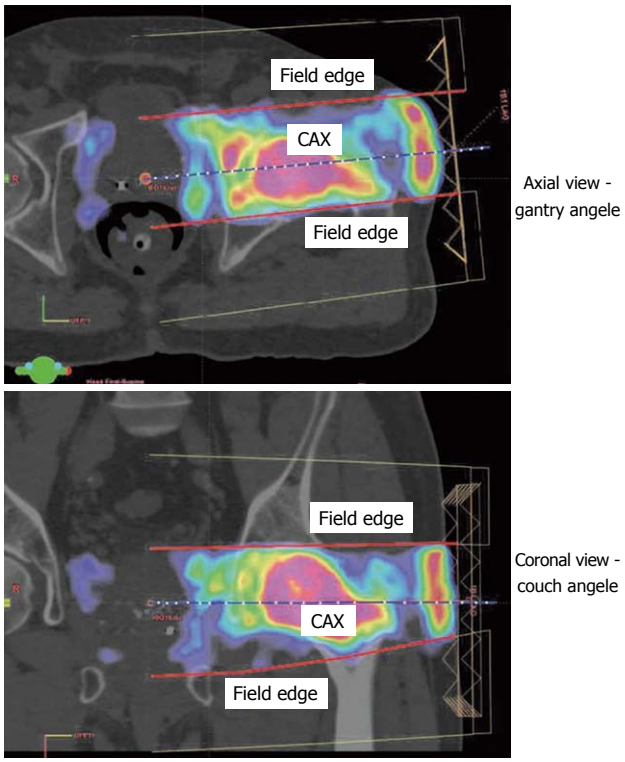

Figure 5 Registered PET images are shown in the axial and coronal views through the prostate. The PET images are fused with the planning computed tomography (CT). The CAX is the central beam axis. The field edge is only extended to the isocenter as provided by the TPS. The isocenter in the lateral direction was set to be the location of the marker-defined path. Good alignment between the field edge and the outer surface of the emitter distribution suggests that no prostate motion occurred after proton beam delivery (Reprinted from[36] with permission from Medical Physics).

margins for treating prostate cancer are sufficient for 86% of the patients. Using this method, the patients with insufficient margins would be noticed during treatment and the margins could be adjusted to account for the extra prostate motion. Again, as with the other studies, offline PET/CT was shown to be a feasible option for proton therapy dosimetry.

CONCLUSION

What method is better, online or offline PET imaging for proton therapy dosimetry? Does the ability to obtain daily activity images in the treatment position outweigh the lack of anatomical data and the smaller field-of-view or is it better to have a good fusion of anatomy and activity with a reduced signal and the possibility of anatomical motion as the patient is transported to the PET/CT scanner? As research progresses into each of these methods, one might develop imaging devices that combine the advantages of both methods. Overall, PET imaging is a robust method for determining the dose to the patient from proton therapy in a noninvasive manner.

REFERENCES

1 **Zullo JR**, Kudchadker RJ, Zhu XR, Sahoo N, Gillin MT. LiF TLD-100 as a dosimeter in high energy proton beam therapy--can it yield accurate results? *Med Dosim* 2010; **35**: 63-66
2 **Hoffman W**, Bienen J, Filges D, Schmitz T. TLD-300 dosimetry in a 175 MeV proton beam. *Rad Prot Dosim* 1999; **85**: 341-343
3 **Hoffman W**. TL dosimetry in high LET radiotherapeutic fields. *Rad Prot Dosim* 1996; **66**: 243-248
4 **Chu TC**, Lin SY, Hsu CC, Li JP. The response of a thermoluminescent dosimeter to low energy protons in the range 30-100 keV. *Appl Radiat Isot* 2001; **55**: 679-684
5 **Oelfke U**, Lam GK, Atkins MS. Proton dose monitoring with PET: quantitative studies in Lucite. *Phys Med Biol* 1996; **41**: 177-196
6 **Litzenberg DW**, Roberts DA, Lee MY, Pham K, Vander Molen AM, Ronningen R, Becchetti FD. On-line monitoring of radiotherapy beams: experimental results with proton beams. *Med Phys* 1999; **26**: 992-1006
7 **Paans AJM**, Schippers JM. Proton therapy in combination with PET as monitor: a feasibility study. *IEEE Trans Nucl Sci* 1993; **40**: 1041-1044
8 **Parodi K**, Enghardt W. Potential application of PET in quality assurance of proton therapy. *Phys Med Biol* 2000; **45**: N151-N156
9 **Vynckier S**, Derreumaux S, Richard F, Bol A, Michel C, Wambersie A. Is it possible to verify directly a proton-treatment plan using positron emission tomography? *Radiother Oncol* 1993; **26**: 275-277
10 **Beebe-Wang JJ**, Dilmanian FA, Peggs SG, Schlyer DJ, Vaska P. Feasibility of Positron Emission Tomography of Dose Distribution in Proton Beam Cancer Therapy. Proceedings of EPAC. Paris, France, 2002
11 **Hishikawa Y**, Kagawa K, Murakami M, Sakai H, Akagi T, Abe M. Usefulness of positron-emission tomographic images after proton therapy. *Int J Radiat Oncol Biol Phys* 2002; **53**: 1388-1391
12 **Tobias CA**, Benton EV, Capp MP, Chatterjee A, Cruty MR, Henke RP. Particle radiography and autoactivation. *Int J Radiat Oncol Biol Phys* 1977; **3**: 35-44
13 **Wilson RR**. Radiological use of fast protons. *Radiology* 1946; **47**: 487-491
14 History of Proton Beam Therapy. Synthesis 2006; Vol. 9, No. 2. Accessed on February 15, 2010. Available from: URL: http://www.ucdmc.ucdavis.edu/synthesis/issues/fall_winter_06-07/features/history.html
15 **Evans R**. The atomic nucleus. Malabar, FL: Krieger Publishing Company, 1955
16 **Jentschke W**. Messungen an harten H-Strahlung. *Physikal Z* 1940; **41**: 524
17 **Nishio T**, Sato T, Kitamura H, Murakami K, Ogino T. Distributions of beta+ decayed nuclei generated in the CH2 and H2O targets by the target nuclear fragment reaction using therapeutic MONO and SOBP proton beam. *Med Phys* 2005; **32**: 1070-1082
18 **Parodi K**, Ferrari A, Sommerer F, Paganetti H. Clinical CT-based calculations of dose and positron emitter distributions in proton therapy using the FLUKA Monte Carlo code. *Phys Med Biol* 2007; **52**: 3369-3387
19 **Schaffner B**, Pedroni E. The precision of proton range calculations in proton radiotherapy treatment planning: experimental verification of the relation between CT-HU and proton stopping power. *Phys Med Biol* 1998; **43**: 1579-1592
20 **Schneider W**, Bortfeld T, Schlegel W. Correlation between CT numbers and tissue parameters needed for Monte Carlo simulations of clinical dose distributions. *Phys Med Biol* 2000; **45**: 459-478
21 **Nishio T**, Ogino T, Sakudo M, Tanizaki N, Yamada M, Nishida G, Nishimura G, Ikeda H. Present proton treatment planning system at National Cancer Center Hospital East. *Jpn J Med Phys Proc* 2000; **20** Suppl 4: 174-177
22 **Hong L**, Goitein M, Bucciolini M, Comiskey R, Gottschalk B, Rosenthal S, Serago C, Urie M. A pencil beam algorithm for

proton dose calculations. *Phys Med Biol* 1996; **41**: 1305-1330
23 **Lin L**, Vargas C, Hsi W, Indelicato D, Slopsema R, Li Z, Yeung D, Horne D, Palta J. Dosimetric uncertainty in prostate cancer proton radiotherapy. *Med Phys* 2008; **35**: 4800-4807
24 **Nishio T**, Miyatake A, Ogino T, Nakagawa K, Saijo N, Esumi H. The development and clinical use of a beam ON-LINE PET system mounted on a rotating gantry port in proton therapy. *Int J Radiat Oncol Biol Phys* 2010; **76**: 277-286
25 **Pawelke J**, Byars L, Enghardt W, Fromm WD, Geissel H, Hasch BG, Lauckner K, Manfrass P, Schardt D, Sobiella M. The investigation of different cameras for in-beam PET imaging. *Phys Med Biol* 1996; **41**: 279-296
26 **Pawelke J**, Enghardt W, Haberer T, Hasch BG, Hinz R, Kramer M, Lauckner K, Sobiella M. In-beam PET imaging for the control of heavy-ion tumour therapy. *IEEE Trans Nucl Sci* 1997; **44**: 1492-1498
27 **Parodi K**, Enghardt W, Haberer T. In-beam PET measurements of beta+ radioactivity induced by proton beams. *Phys Med Biol* 2002; **47**: 21-36
28 **Parodi K**, Ponisch F, Enghardt W. Experimental study on the feasibility of in-beam PET for accurate monitoring of proton therapy. *IEEE Trans Nucl Sci* 2005; **52**: 778-786
29 **Nishio T**, Ogino T, Nomura K, Uchida H. Dose-volume delivery guided proton therapy using beam on-line PET system. *Med Phys* 2006; **33**: 4190-4197
30 **Enghardt W**, Parodi K, Crespo P, Fiedler F, Pawelke J, Pönisch F. Dose quantification from in-beam positron emission tomography. *Radiother Oncol* 2004; **73** Suppl 2: S96-S98
31 **Parodi K**, Crespo P, Eickhoff H, Haberer T, Pawelke J, Schardt D, Enghardt W. Random coincidences during in-beam PET measurements at microbunched therapeutic ion beams. *Nucl Instr Meth* 2005; **545**: 446-458
32 **Parodi K**, Paganetti H, Cascio E, Flanz JB, Bonab AA, Alpert NM, Lohmann K, Bortfeld T. PET/CT imaging for treatment verification after proton therapy: a study with plastic phantoms and metallic implants. *Med Phys* 2007; **34**: 419-435
33 **Lin L**, Hsi W, Indelicato D, Vargas C, Flampouri S, Slopesema R, Keole SR, Li Z, Yeung D, Palta JR. In vivo verification of dose delivery to prostate cancer by utilizing PET/CT images taken after proton therapy. *Int J Radiat Oncol Biol Phys* 2008; **72** Suppl 1: S144
34 **Parodi K**, Paganetti H, Shih HA, Michaud S, Loeffler JS, DeLaney TF, Liebsch NJ, Munzenrider JE, Fischman AJ, Knopf A, Bortfeld T. Patient study of in vivo verification of beam delivery and range, using positron emission tomography and computed tomography imaging after proton therapy. *Int J Radiat Oncol Biol Phys* 2007; **68**: 920-934
35 **Nishio T**, Miyatake A, Inoue K, Gomi-Miyagishi T, Kohno R, Kameoka S, Nakagawa K, Ogino T. Experimental verification of proton beam monitoring in a human body by use of activity image of positron-emitting nuclei generated by nuclear fragmentation reaction. *Radiol Phys Technol* 2008; **1**: 44-54
36 **Hsi WC**, Indelicato DJ, Vargas C, Duvvuri S, Li Z, Palta J. In vivo verification of proton beam path by using post-treatment PET/CT imaging. *Med Phys* 2009; **36**: 4136-4146
37 **Tomitani T**, Pawelke J, Kanazawa M, Yoshikawa K, Yoshida K, Sato M, Takami A, Koga M, Futami Y, Kitagawa A, Urakabe E, Suda M, Mizuno H, Kanai T, Matsuura H, Shinoda I, Takizawa S. Washout studies of 11C in rabbit thigh muscle implanted by secondary beams of HIMAC. *Phys Med Biol* 2003; **48**: 875-889
38 **Mizuno H**, Tomitani T, Kanazawa M, Kitagawa A, Pawelke J, Iseki Y, Urakabe E, Suda M, Kawano A, Iritani R, Matsushita S, Inaniwa T, Nishio T, Furukawa S, Ando K, Nakamura YK, Kanai T, Ishii K. Washout measurement of radioisotope implanted by radioactive beams in the rabbit. *Phys Med Biol* 2003; **48**: 2269-2281
39 **Ferrari A**, Sala PR, Fassò A, Ranft J. FLUKA: a multi-particle transport code. CERN yellow report, INFN/TC_05/11, SLAC-R-773. Geneva, 2005
40 **Conti M**, Bendriem B, Casey M, Chen M, Kehren F, Michel C, Panin V. First experimental results of time-of-flight reconstruction on an LSO PET scanner. *Phys Med Biol* 2005; **50**: 4507-4526
41 **Parodi K**, Bortfeld T. A filtering approach based on Gaussian-powerlaw convolutions for local PET verification of proton radiotherapy. Phys Med Biol 2006; 51: 1991-2009

S- Editor Cheng JX **L- Editor** Negro F **E- Editor** Zheng XM